RSC Advances

ROYAL SOCIETY OF CHEMISTRY

www.rsc.org/advances

Reactive Molecular Dynamics Simulation of the Pyrolysis and Combustion of Benzene: Ultrahigh Temperature and Oxygen-Induced Enhancement of Initiation Pathways and Their Effect on Carbon Black Generation

Xiaona Dong[a], Yude Fan[b], Xing Fan[b], Yushi Wen[b,] *

[a]*College of Mathematics and Computer Science, Mianyang Normal University, Mianyang, Sichuan 621000, China.*

[b]*Institute of Chemical Materials, China Academy of Engineering Physics (CAEP), P. O. Box 919-326, Mianyang, Sichuan 621900, China.*

Abstract The pyrolysis and combustion mechanisms of benzene under different chemical environment and temperatures were investigated by reactive force field based molecular dynamics (ReaxFF MD) simulation using two systems, pure benzene and a mixture of benzene and oxygen gas. The chemical behaviors of this system were investigated under ultrahigh temperature that can be induced by high-energy density laser and compared to those at high temperature. According to some experimental data, we assume that ultrahigh temperature can be used to mimic laser irradiation. The conclusions of this simulation are as follows. First, the ReaxFF MD simulations showed that the decomposition rates of benzene were significantly accelerated by laser irradiation or in the presence of oxygen. Second, additional initiation pathways were opened up by these two factors. The primary initiation pathway involves only the hydrogen atom loss in the pyrolysis of benzene at 3,000 K, and the initiation pathways become much more complicated after laser irradiation or the involvement of oxygen. Third, the ReaxFF MD simulations formed reasonable carbon black (CB) texture of various sizes in the pyrolysis of benzene, and we also focused on the evolution of the texture of CB. The calculation results of the final gaseous products, hydrocarbons, and the formation of CB are in a good agreement with the literature. This study provides a better understanding of the initiation mechanisms of the pyrolysis and combustion of benzene under extreme conditions.

Keywords: pyrolysis and combustion, benzene, carbon black generation, ReaxFF, molecular dynamics simulation

1 Introduction

Combustion and pyrolysis are both ubiquitous and the most significant current interest in power source applications, storage, and engineering science. Therefore, significant efforts have been directed to investigate the evolution, reaction mechanism, and kinetics of the pyrolysis and combustion of hydrocarbons, alternative fuels, biofuels, etc. [1–14]. Carbon black (CB) is one of the most common products of the

combustion and pyrolysis of hydrocarbons. The past four decades have witnessed the rapid development of the study on CB due to its widespread application and distinct properties. The world production of CB is ~10 Mt per year [15]. CB can be used as antistatic plastics, electrically conductive agents in plastics [16, 17] and is extensively used as a catalyst support in the proton exchange membrane fuel cells [18–20] due to its excellent electrical conductivity. It also can be used as reinforcing compounds in rubbers [21, 22] as a valuable elastomer filler, because of its low thermal expansion coefficient and excellent heat-, chemical-, and weather resistance [23]. It is also a good candidate for the thermal interface pastes, because of its excellent thermal conductivity [24, 25].

In general, different manufacturing processes of CB share common procedures, i. e., liquid or gaseous hydrocarbons are decomposed at elevated temperatures under oxygen deficient atmosphere, i. e., pyrolysis or partial combustion [26]. Nowadays, CB is mainly produced by the furnace back process, where hydrocarbons are partially combusted and immediately quenched with water [27, 28]. The reaction conditions including rates of heating, heat treatment temperature, soak time, and ambient gases affect the pyrolysis process and the products [29]. For instance, significant differences have been observed in the chemical composition of diesel engine and exhaust soots, because of their differences in the quenching and post quenching environment of soot [30]. The sorts of feedstock can also be of crucial importance for the generation of CB. Therefore, in recent years, significant attention has been focused on the oxidation mechanism of ordinary hydrocarbons including alkenes, alkynes, aromatics, and so on.

For instance, the pyrolysis and combustion of *n*-dodecane was studied by Li, *et al*. [12]; the mechanism and kinetics for the initial steps of pyrolysis and combustion of 1,6-dicyclopropane-2,4-hexyne was investigated by Liu *et al*. [13] using reactive molecular dynamic methods; Li *et al*. [31] studied the oxidation of toluene at high temperatures, and the simulations by Qian *et al*. [14] showed the formation of fullerene during the combustion of benzene.

Benzene is an aromatic hydrocarbon, a natural constituent of crude oil and is one of the most elementary petrochemicals. Nevertheless, its presence in some industrial materials such as gasoline is limited in most countries, because of its severe environmental and health effects. Moreover, most nonindustrial applications have been limited by benzene's carcinogenicity [32]. The combustion of benzene produces harmful volatile organic compounds (VOCs), namely, the products of benzene combustion in incomplete hydrocarbon oxidation or pyrolysis include the polycyclic aromatic hydrocarbons and eventually the soot or graphitized CB. To decrease the VOCs formation, a detailed understanding of the reaction pathways of benzene under high temperature conditions is essential. The combustion of benzene at flame temperature or catalytic combustion of benzene has attracted significant attention [33–38].

The pyrolysis of benzene can also occur under the laser irradiation, during which some useful nanomaterials can be obtained. For example, carbon nanoparticles were produced by the irradiation of NIR femtosecond (fs) laser pulses to a benzene/water bilayer[39]. C60 and C70 structures were obtained during the pyrolysis of

benzene-based chemical compound induced by the laser irradiation, where the C/O ratio affects the ratio of production of C60 and C70 [40]. The increase in the C/O ratio increased the productions of C60 and C70, in particularly of C60.

Although significant studies have been performed on the mechanisms and kinetics of the pyrolysis and combustion of benzene at lower temperatures such as <2,500 K[33–38], the exact nature of the chemical process of the pyrolysis and combustion of benzene at ultrahigh temperatures such as under the loading of high-energy density laser is barely reported. The differences between low temperature and high temperature cases and the type and growth of naonmaterials observed during the pyrolysis at high temperatures have not been studied. All these questions are still not fully understood. However, because of ultrahigh temperature and very short reaction time, the pyrolysis and combustion of hydrocarbon (e. g., benzene) by experiment alone is very challenging. Therefore, the reactive molecular dynamics simulation becomes a feasible method to deal with the issue.

In this study, the initiation mechanisms and chemical evolution of the pyrolysis and combustion of benzene were investigated by the ReaxFF based reactive molecular dynamics simulations (RMD). A previous study on the combustion of benzene using ReaxFF MD[14], where the H atoms were removed during the combustion as soon as they combined into H_2 gas, showed the formation of some compounds such as fullerene, and our results are in agreement with this study. Yet this study did not focus on the initial decomposition of benzene and the chemical evolutions on the existence of H atoms, which is one of our objectives. The combustion of other hydrocarbon

such as n-dodecane[12] is also reported. Their study focused on the reaction pathway for the decomposition of benzene and did not mention the carbon black formation. In this study, the pyrolysis and combustion behaviors under ultrahigh temperature (7,000 K) which can be induced by high-energy density laser irradiation were compared to those produced under normal high-temperature loading (3,000 K). Laser-heated materials such as carbon-based compound can be turned into plasma, and the temperatures can reach to 10 thousands of K [41, 42]. Ultrahigh temperature was used to mimic a circumstance under laser irradiation. First, from the ReaxFF MD simulations, the initiation mechanisms of the pyrolysis of benzene were found to be dependent on temperature and chemical environment. Second, the ReaxFF MD simulations led to a reasonable CB texture of various sizes formed in the pyrolysis of benzene, focusing on the CB texture evolution. Third, O_2 was added to provide a benzene/O_2 ratio of 2/3 to investigate the effect of added oxygen. The dissociation rates of benzene in the pure benzene system and benzene in the presence of O_2 system were also analyzed and compared.

The simulation results were compared to the previous experimental literature observations[1, 33–38, and 43]. To some extent, an agreement between the simulation and experimental data was achieved.

2 Methodologies

2.1 Models

Both the pyrolysis of benzene and formation of carbon black have been modeled in a condensed-phase environment at a density corresponding to the density of liquid

benzene at room temperature, i. e., 0.879 g/cm^3. A cell of benzene composed of 100 benzene molecules (1,200 atoms) was used to study the pyrolysis of pure benzene. Another cell composed of 100 benzene molecules and 150 O_2 molecules (1500 atoms) was used to study the partial combustion of benzene. The scale effect on the simulation result was investigated. For instance, a calculation was performed on a cell of benzene using a system of 3,600 atoms for 1,000 ps, and the result in our simulation time was found to be similar to that of a smaller system of 1,200 atoms.

2.2 Calculations

A newly developed molecular reactive force field ReaxFF was used to simulate the pyrolysis and combustion of benzene. The validity of ReaxFF to benzene and O_2 was confirmed by the previous studies [13, 14, 31, 44–46]. After the relaxation, the two cells were subjected to different high-temperature simulations under canonical particle number, volume, and temperature (NVT) conditions with the multiple Nosé−Hoover thermostat method [47]. A total of four simulations were performed. The information on the temperatures and time of the NVT-MD molecular dynamic simulations is listed in Table 1. The value of 3,000 K was used to simulate the initial or subsequent high-temperature pyrolysis or combustion; 7,000 K temperature was used to simulate the ultrahigh temperature effect induced by laser irradiation. In Cases 1 and 2, the temperature of 7,000 K was only present for 20 ps and after that the temperature was decreased to 3,000 K.

Table 1 The information of the temperatures and time of NVT simulations

NO. of	Starting temperature	The cell	Continuous	To simulate

CASE	and time/ K		temperature/K	
1	7,000 (for 20 ps)	Benzene	3000 (for 6 ns)	laser induced pyrolysis
2		Benzene + O_2	3000 (for 2 ns)	laser induced combustion
3	3,000 (for 20 ps)	Benzene	3000 (for 2 ns)	pyrolysis
4		Benzene + O_2		combustion

The ReaxFF is a DFT based reactive force field. The cleavage and formation of chemical bonds can be accurately described during reactions [48]. In this study, the LAMMPS software package was used [49, 50] to perform all the simulations.

2.3 Dynamic Trajectory Analyses

For each simulation, a time step of 0.1 fs was assigned, and the dynamic trajectories including atomic positions and velocities were recorded every 1 ps and analyzed by a FORTIAN scripts based on the ideas of Strachan *et al*. [51] to provide information on the chemical reactions. The bond-order cut off values for each pair of elements in ReaxFF can be checked elsewhere [13, 14, 31].

3 Results and Discussion

3.1 Initial steps of the decomposition for oxidation of benzene

In this study, the results of the initial products and the products produced on a longer time scale are presented. The initial products are produced from the earliest decomposition of benzene molecules. The initial products generated very early and are commonly very unstable. They react in a very short time. The products produced on a longer time scale are the results of the evolutions of the initial products. These products are more stable than the initial products and their amounts either kept

increasing or were stable during a reasonably long time.

Table 2 The initial products and the moments they generated of four NVT simulations

Case 1		Case 2		Case 3		Case 4	
Products	Time, ps	Products	Time, ps	Products	Time, ps	Products	Time, ps
C_6H_5	1.00	C_6H_5	1.00	C_6H_5	25.00	$C_6H_6O_2$	1.00
H	1.00	H	1.00	H	25.00	C_6H_5	7.00
C_2H_2	2.00	$C_6H_6O_2$	1.00			H	7.00
C_4H_4	2.00	C_2H_2	2.00			C_2H_2	12.00
		C_4H_4	2.00				
		$C_3H_4O_2$	2.00				
		C_3H	2.00				
		HO_2	2.00				
		C_6H_7	2.00				
		O	2.00				

The detailed reaction mechanisms extracted from the dynamic trajectories are presented here. The initial products of the four cases are shown in Table 2. For Case 1, C_6H_5, and H were observed within 1 ps; C_2H_2 and C_4H_4 were observed within 2 ps. Therefore, the pyrolysis pathway of benzene observed in the ReaxFF NVT-MD simulation at T = 7,000 K can be represented by Scheme 1 (Table 3), including the hydrogen atom loss and cycloreversion. Case 2 have the same products as C_6H_5, H, C_4H_4, and C_2H_2 on the same steps of reaction as that of Case 1. Besides, the formation of $C_6H_6O_2$ was observed in 1 ps. $C_3H_4O_2$, C_3H, HO_2, C_6H_7, and O were observed within 2 ps. Mechanisms of the initial pyrolysis and combustion was complicated by adding oxygen. Therefore, the pathway of benzene and O_2 system observed in the ReaxFF NVT-MD simulation at T = 7,000 K can be shown by Scheme 2 including hydrogen atom loss and cycloreversion and from the middle of the ring after adding O_2. For case 3, the initial products include C_6H_5 and H, which are much simpler. Lower temperature and pure chemical components lead to a simple mechanism of the

initial pyrolysis simply involving hydrogen atom loss, as shown in Scheme 3. The products of Case 4 include $C_6H_6O_2$, C_6H_5, H, and C_2H_2. The addition of oxygen affects the mechanisms of the initial pyrolysis by adhering to the molecule of benzene. Therefore, the pathway of Case 4 can be shown by Scheme 4, including hydrogen atom loss and cycloreversion of the ring into three parts evenly.

Table 3 Initial reaction observed in the pyrolysis or combustion. Times observed corresponding to the frequency of the mechanism observed..

Name	Reactions	Temperature	Reactants	Times Observed
Scheme 1	$C_6H_6 \longrightarrow C_6H_5 + H$ $C_6H_6 \longrightarrow C_4H_4 + C_2H_2$	7000 K	Neat Benzene	> 20
Scheme 2	$C_6H_6 \longrightarrow C_6H_5 + H$ $C_6H_6 \longrightarrow C_4H_4 + C_2H_2$ $C_6H_6 + O_2 \longrightarrow C_6H_6O_2$ $C_6H_6O_2 + C_6H_6 \longrightarrow C_3H_4O_2 + C_3H + C_6H_7$ $C_6H_6O_2 \longrightarrow C_6H_5 + HO_2$ $O_2 \longrightarrow O + O$	7000 K	Benzene & O_2	> 7
Scheme 3	$C_6H_6 \longrightarrow C_6H_5 + H$	3000 K	Neat Benzene	> 25
Scheme 4	$C_6H_6 \longrightarrow C_6H_5 + H$ $C_6H_6 \longrightarrow 3C_2H_2$	3000 K	Benzene & O_2	> 12

From the initial products of these cases, at higher temperatures, the mechanism is more complicated. In Case 3, at low temperature and pure chemical component, only one pathway involving the hydrogen atom loss exists for the decomposition of benzene. In Case 1, of the same chemical component, at a much higher temperature, decomposition follows an alternative pathway, i. e., cycloreversion. The comparison of Cases 2 and 4 also support this statement.

Another conclusion is that the mechanism of the initial pyrolysis becomes more complicated by adding oxygen. Cases 1 (two pyrolysis pathways) and 2 (three pyrolysis pathways) are both at 7,000 K; however, the initial steps of Case 2 are more complicated, because of the presence of oxygen. The comparison of Cases 3 (one pyrolysis pathway) and 4 (two pyrolysis pathways) also support this statement.

Benzene decomposition pathways at lower temperatures in previous studies [1, 33–38] are mainly hydrogen atom loss, forming less atoms rings such as five-membered carbon rings[43] and then the decomposition of the rings, as well as a certain branching ratio of benzene cycloreversion. However, the cycloreversions need much longer induction time and proceed in many steps in longer time. At higher temperatures, the cycloreversions become more important and less atoms rings are fewer. The cycloreversions of benzene at higher temperature need much shorter induction time and proceed in fewer steps, i. e., benzene breaks into three C_2H_2 in 1 ps, which in our time resolution for one step.

C_6H_6 -> C_6H_5 + H reaction needs to overcome the energy barrier of a single bond, a C–H bond with bond dissociation energy (BDE) of 448.4 kJ/mole [52]. C_6H_6 -> C_4H_4 + C_2H_2 reaction needs to overcome the energy barrier of a sp2-sp2 C–C bond in benzene with a bond length of 140 pm. The BDE can be calculated by the method of Andreas, [53] and was found to be 614.5 kJ/mole. The later needs higher energy to break than the former. Therefore, at lower temperature C_6H_6 -> C_6H_5 + H reaction dominates unimolecular decomposition pathway of benzene. The competing channel to C_4H_4 + C_2H_2 becomes more dominating as the temperature increases.

3.2 Temperature and chemical environment effect on the decomposition rates of benzene

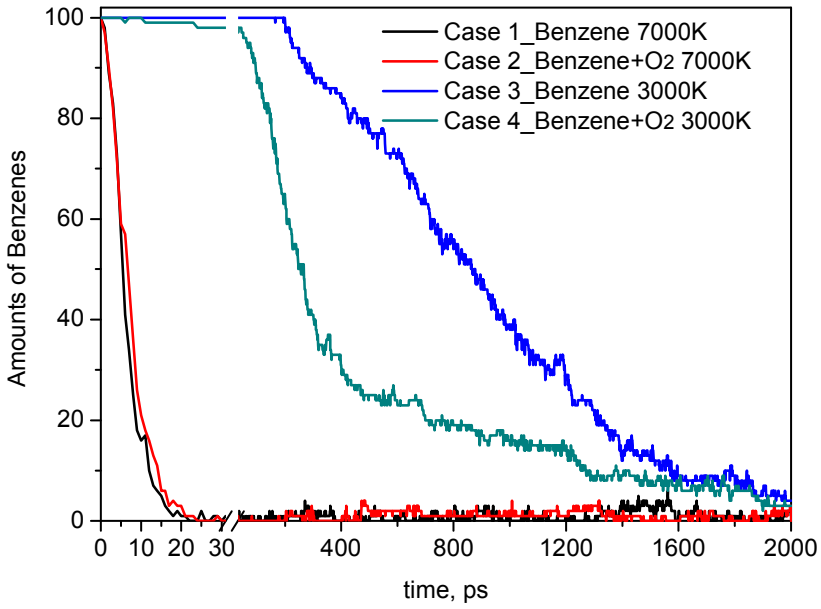

Figure 1 Decay evolutions of benzene in four simulations.

Decay evolutions of benzene in the four cases are shown in Figure 1. The decompositions of benzene in Cases 1 and 2 basically completed in 30 ps, whereas those in Cases 3 and 4 completed in 2,000 ps. The decomposition rates under 7,000 K were obviously much higher than those under 3,000 K. The decomposition rates of Cases 1 and 2 were essentially the same, and the decomposition rates of Case 4 are more than that of Case 3, indicating that the oxygen gas accelerated the reaction of benzene at lower temperature. For a much higher temperature, the acceleration of oxygen was not obvious because of an originally very high reactivity.

Both Cases 3 and 4 shows obvious induction time for the decomposition of C_6H_6. The induction time of Case 4 (15 ps) is shorter than that of Case 3 (350 ps), which

should be the result of the enhancement of the reaction activity because of the presence of O_2.

The induction time arise from the overcoming of the reaction barrier for the benzene decomposition. The internal energy initially evenly distributed amongst the various degrees of freedom needs to be redistributed so that there is enough energy in the mode that reflects decomposition so that the barrier can be overcome (e.g., a C-H stretch mode for the C_6H_6 -> C_6H_5 + H reaction). The induction times in Cases 1 and 2 are much shorter, because much higher temperatures are applied to these systems.

3.3 Evolutions of further chemical reactions and the effect of O_2 on the pyrolysis/combustion of benzene

The evolutions of main chemical products in the early stages of the decomposition under aforementioned temperatures and chemical atmosphere were analyzed and shown in Figures 2–5.

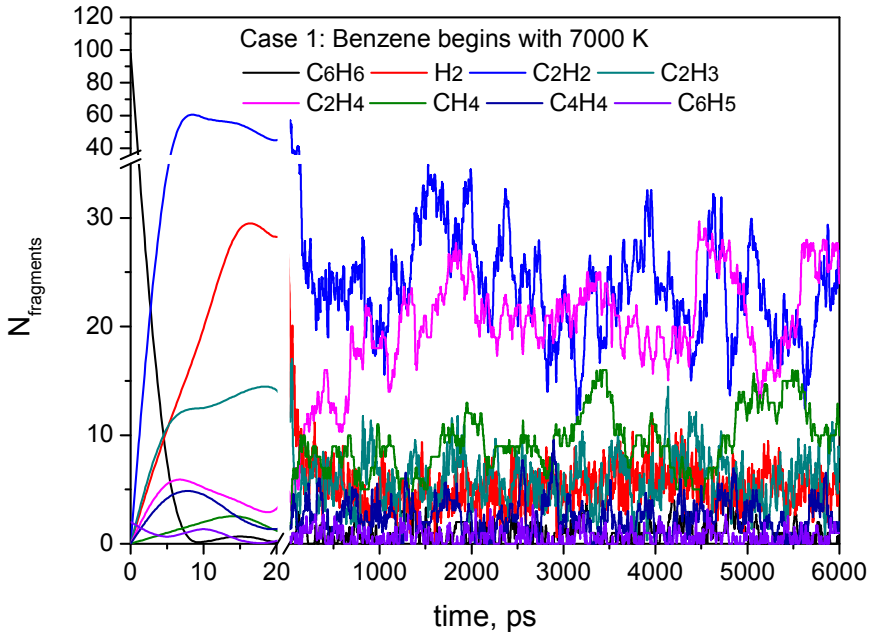

Figure 2 The evolution of products in the decomposition of benzene during the NVT-MD simulation at T = 3,000 K after 20 ps stimulation at T = 7,000 K. The initial number of C_6H_6 molecules is 100. At least 50 hydrocarbons (from C1 to C38) were observed, and some of which are in small ratios and not listed in the figures to avoid crowded lines.

Figure 2 (neat benzene, 7,000 K for 20 ps and then 3,000 K for 6 ns) shows that C_2H_2 (blue line), C_2H_4 (pink line), CH_4 (green line), and H_2 (red line) are created rapidly at the beginning of early 20 ps simulation. At ~50 ps, the rapid increase in the H_2 stops, and a sharp decrease is observed. For other three products, C_2H_2, C_2H_4, and CH_4, a plateau followed after a slight decrease.

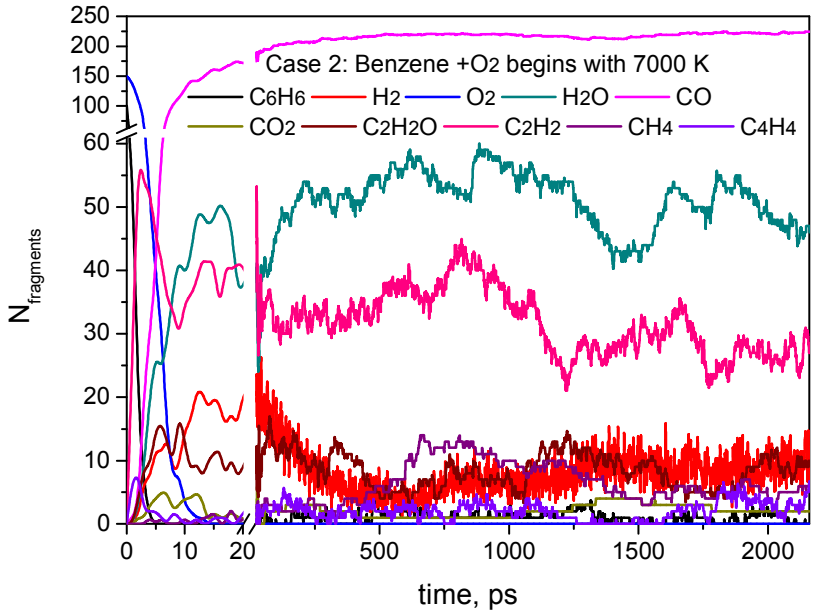

Figure 3 Products evolution of benzene in O_2 atmosphere during the NVT-MD simulation at T = 3,000 K after 20 ps stimulation at T = 7,000 K. The initial number of C_6H_6 molecules is 100. At least 10 hydrocarbons (from C1 to C7) were observed, and some of which are in small ratios and not listed in the figures to avoid crowded lines.

Figure 3 (benzene in O_2 atmosphere, 7,000 K for 20 ps and then 3,000 K for 2.3 ns) shows that CO (pink line), H_2O (dark cyan line), C_2H_2 (red line), C_2H_4 (yellow line), and H_2 (dark red line) are created rapidly at the beginning of early 20 ps simulation. At ~100 ps, the rapid increase in H_2 stops, and a sharp decrease is observed. For other four products, CO, H_2O, C_2H_2, and C_2H_4, a plateau is observed after a slight increase. The comparison of Figures 3 and 4 shows that under the same temperature histories, both C_2H_2 and C_2H_4 are the main products. The presence of O_2 induces the main products of CO and H_2O and also decreases the average size of products.

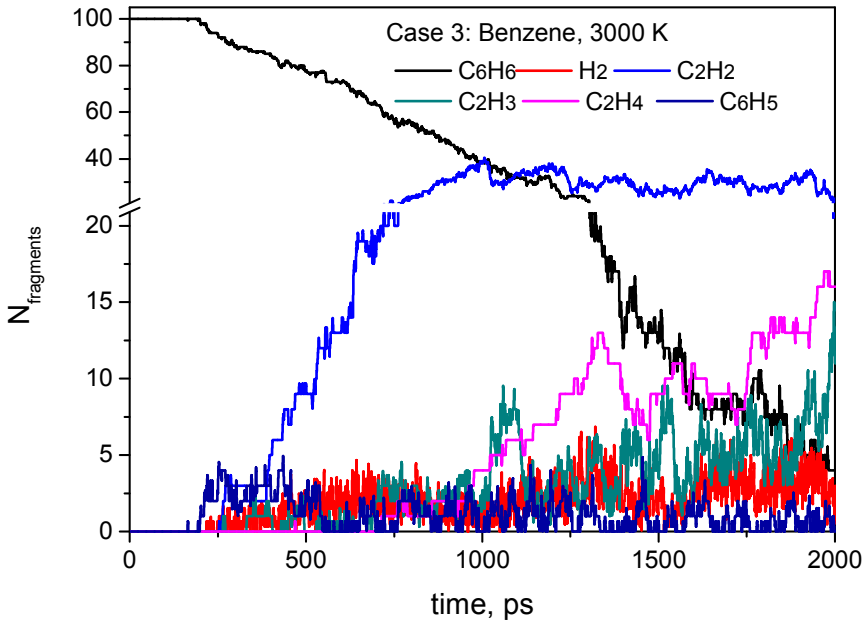

Figure 4 The evolution of products in the decomposition of benzene during the NVT-MD simulation at T = 3,000 K. The initial number of C_6H_6 molecules is 100. At least 25 hydrocarbons (from C1 to C17) were observed, and some of which are in small ratios and not listed in the figures to avoid crowded lines.

Figure 4 (neat benzene, 3,000 K for 2 ns) shows that the decomposition starts at ~350 ps and then gradually decreases. C_2H_2 (blue line) is the first and major product, generated in ~350 ps and reached its largest amount in ~1,000 ps. After that the amount of C_2H_2 was kept constant. C_2H_4 (pink line) and C_2H_3 (dark cyan line) are created at ~500 ps and increased gradually to high amounts.

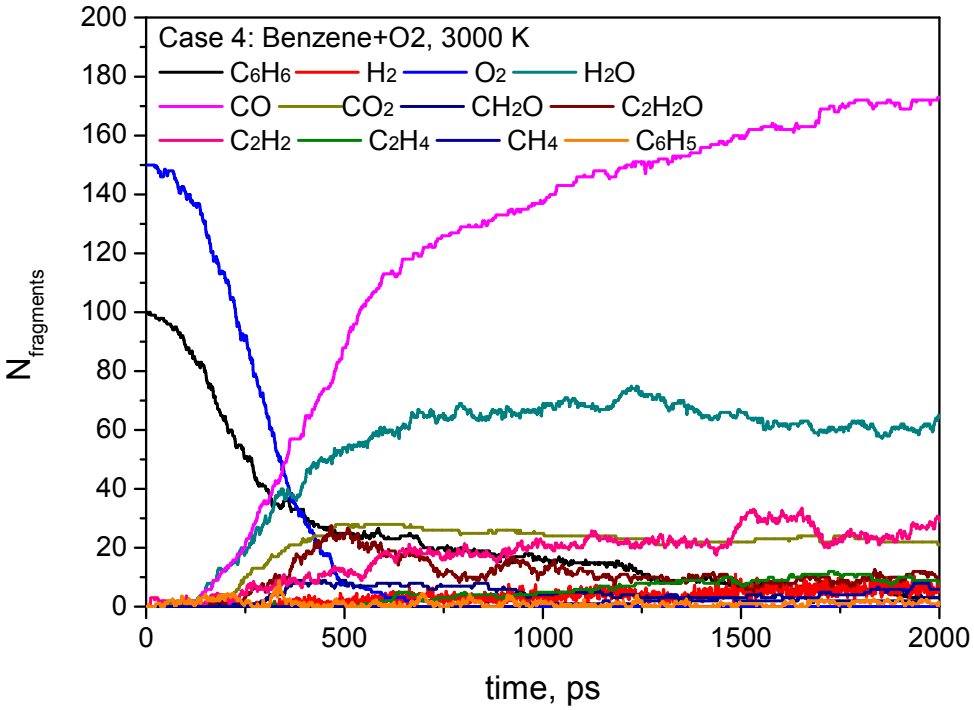

Figure 5 The evolution of products in the decomposition of benzene in the presence of O_2 atmosphere during the NVT-MD simulation at T = 3,000 K. The initial number of C_6H_6 molecules is 100. At least 20 hydrocarbons (from C1 to C15) were observed, and some of which were in small ratios and not listed in the figures to avoid crowded lines.

Figure 5 shows the decomposition of benzene in the presence of O_2 atmosphere at 3,000 K for 2 ns, indicating that the decomposition of benzene and O_2 started very early and then gradually decreased. The levels of O_2 and benzene decreased to very low at ~500 and 1,500 ps, respectively. CO (pink line), H_2O (dark cyan line), CO_2 (yellow line), C_2H_2 (dark pink line, the lower one) are formed rapidly at the beginning of the simulation. After ~500 ps, plateaus followed after the increase. The products of Case 4 are very similar to those of Case 2. The presence of O_2 also induces the formation CO and H_2O as the main products and also decreased the average size of the products, indicating that the effect of the chemical atmosphere is very significant, probably larger than the effect of the temperature.

In summary, the analysis of the initial decomposition reactions and the products

of benzene shows the dependence on temperature and chemical atmosphere: (1) higher temperatures (7,000 K simulating laser ablation) resulted in much higher decomposition rate. In both Cases 1 and 2, benzenes decomposed in 20 ps, and further reactions quickly reached to equilibrium. (2) The presence of O_2 significantly affects the final products.

In the experimental study of the benzene oxidation by Chai *et al.*[43], acetylene was a major hydrocarbon intermediate, and their result is consistent with our result of all the four cases. For the oxidation of benzene at low pressure (45 mbar) by Detilleux[54], fifteen chemical species were detected in benzene flames, including final gaseous products (O_2, CO_2, H_2O, CO, and H_2) and ten hydrocarbons (ranging from C1 to C6). Yang *et al.* [55] studied the oxidation of the premixed benzene/oxygen/argon flame with tunable synchrotron photoionization and found that the hydrocarbons include CH_3, C_2H, C_2H_3, C_2H_5, C_3H, C_3H_3, C_3H_5, C_4H, C_4H_3, C_4H_5, C_4H_7, C_5H_3, C_5H_5, C_5H_7, C_6H_5, C_6H_5O, C_7H_7, and C_9H_7 in the flame. CO, CO_2, H_2, and H_2O were also observed in the final gaseous products. Moreover, the isomers of some PAHs were also identified. Most of these free radicals were obtained in our simulations. Some PAHs or CB were also identified in our results. In summary, our calculation results of the final gaseous products and hydrocarbons~~, the formation of CB~~ are in a good agreement with the literature.

3.4 CB texture evolution during the pyrolysis or combustion

The formation of CB was observed during the pyrolysis or combustion of benzene and benzene in the presence of O_2. The CB texture evolutions in Cases 1–4

are shown in Figures 6–9. The CB texture evolutions during the pyrolysis of pure benzene and benzene in the presence of O_2 after laser irradiation at 7,000 K are shown in Figures 6 and 7, respectively, indicating that in both the cases, benzene gradually decomposed, and then the carbon atoms gathered together to form CB. The differences between the two cases are the size of CB and the time required for its formation. The CB formed in the pure benzene is larger than that formed in benzene in the presence of O_2. Moreover, the generation of the former needs shorter time. After careful investigation, the CBs were found to mainly consist of six-membered ring systems. The carbonaceous enrichment occurs after the carbon atoms escape from the benzene molecules. Nucleus appears when the unstable network becomes aromatic. Moreover, the carbon atoms adjust their positions and approximate forms the six-membered ring systems. During this process, the CB structures of the graphite-like lamellar are built and fly over in the simulation box, absorbing more escaped carbon atoms and a few hydrogen atoms, resulting in further growth.

Fig. 7 (7,000K in the presence of O_2) shows that at 500 ps a polycyclic aromatic hydrocarbon forms (lower right), which then reacts later. It is a critical step in mechanism for rapid growth of aromatic structures. In absence of O_2, the polycyclic aromatic hydrocarbon formed will eventually grow into graphitized CB, similar to that shown in Fig. 6 (7,000 K in the absence of O_2). In the presence of O_2, O_2 attacks the polycyclic aromatic hydrocarbons once it forms, and therefore formation of big graphitized CB is more difficult.

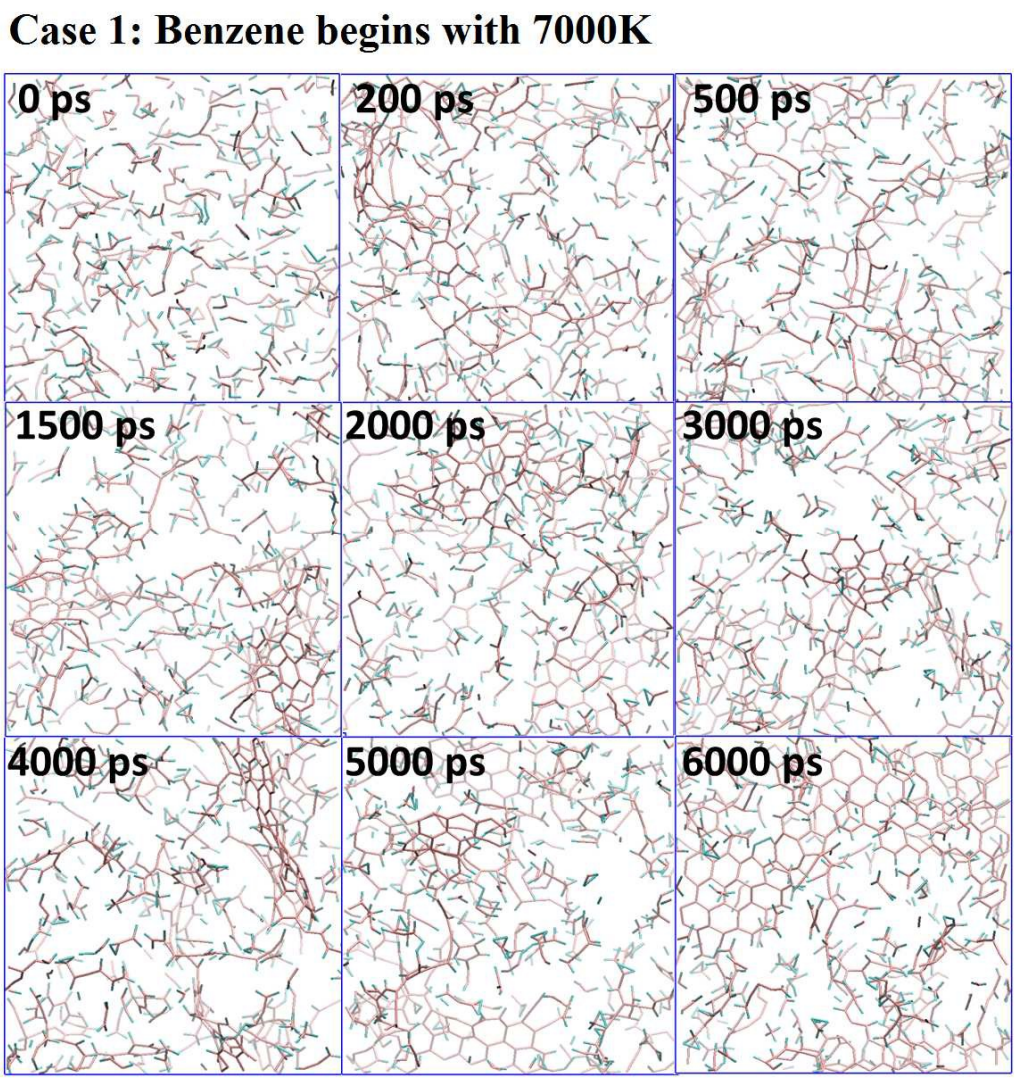

Figure 6 Snapshots of benzene during the NVT-MD simulation at T = 3,000 K after 20 ps stimulation at T=7,000 K

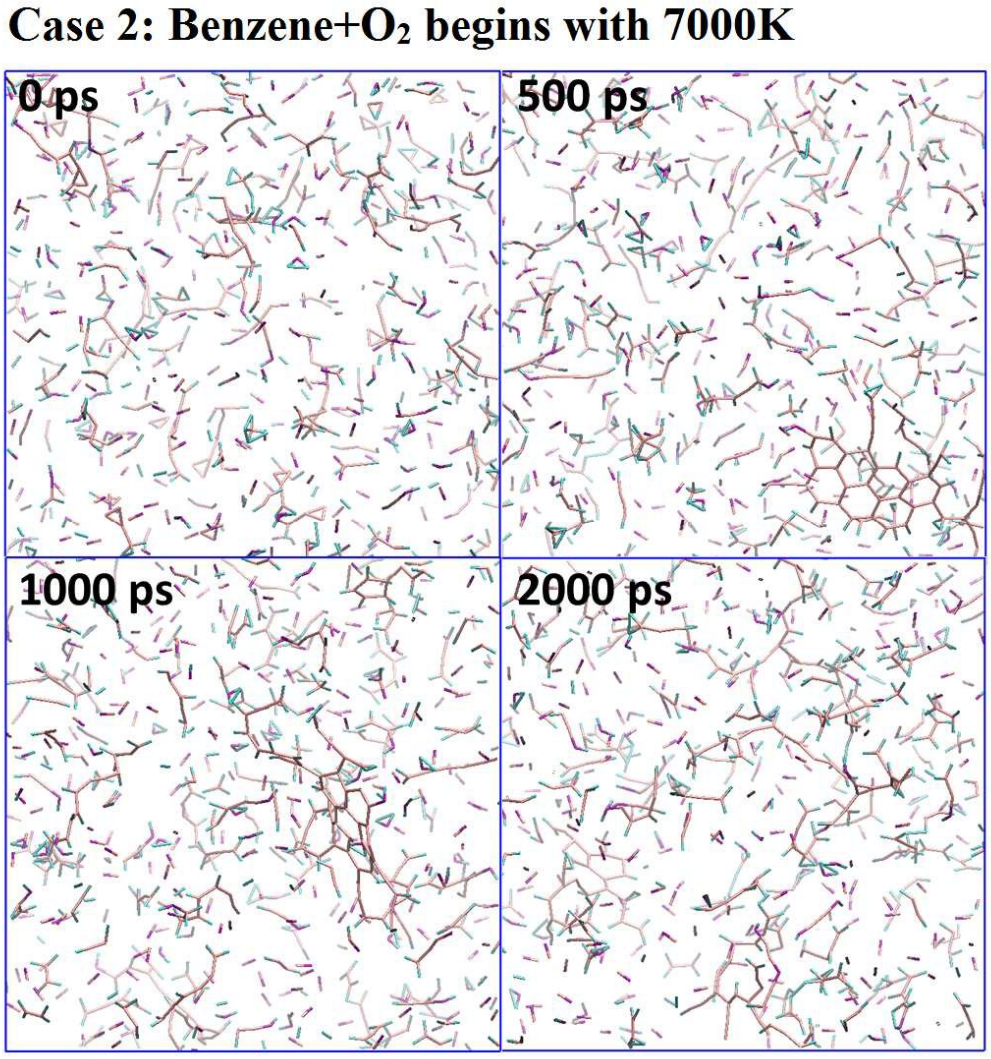

Figure 7 Snapshots of the decomposition of benzene in O_2 atmosphere during the NVT-MD simulation at T=3, 000 K after 20 ps stimulation at T=7,000 K

The CB texture evolutions during the pyrolysis of the pure benzene and benzene in the presence of O_2 at 3,000 K are shown in Figures 8 and 9, respectively. The pictures also show that in both the cases, the benzene molecules gradually decomposed, and then the carbon atoms gathered together to form CB. The reaction at 3,000 K is much slower than that at 7,000 K, and the formation of CB needs more time.

The difference between Cases 3 and 4 are also the size of the CB and the time

required for its formation. The size of the CB formed in the pure benzene is larger than that formed in benzene in the presence of O_2 as well as at 3,000 K. Moreover, the generation of the former needs shorter time.

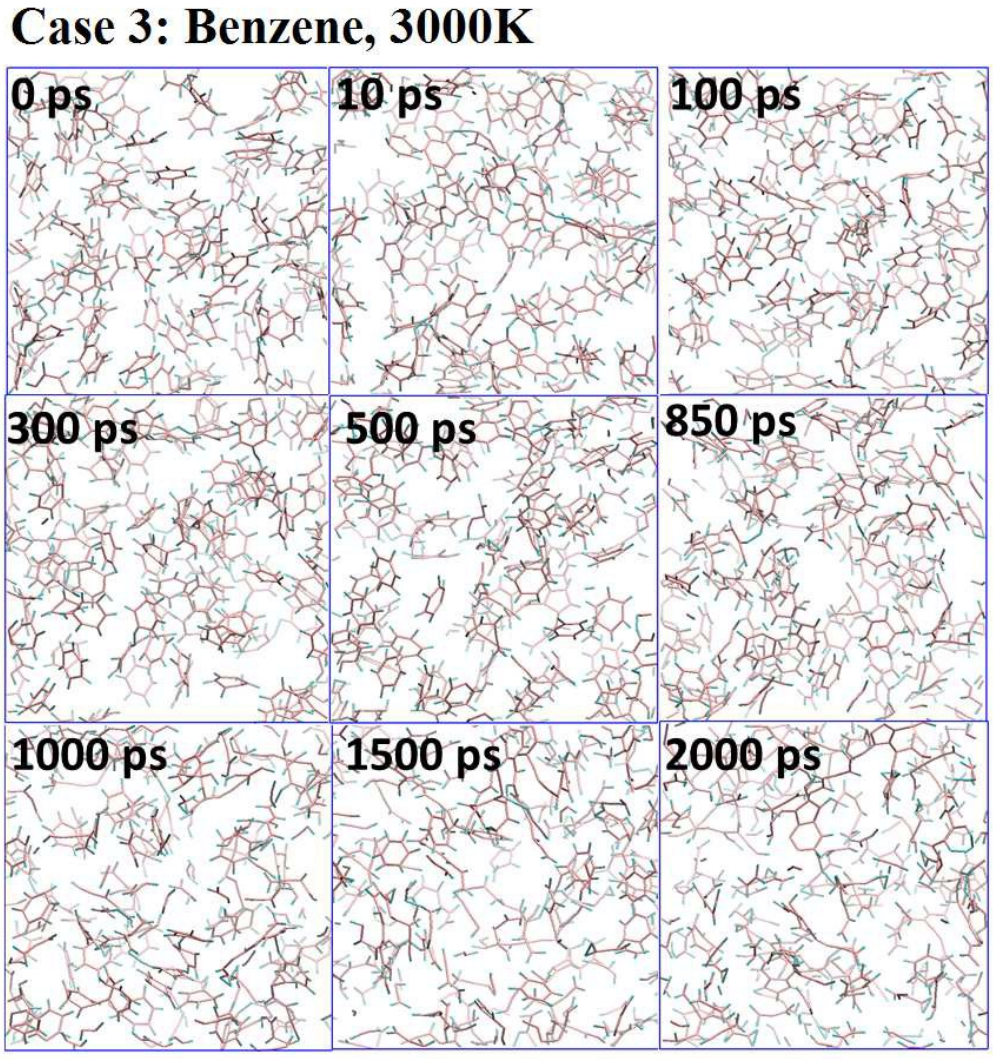

Figure 8 Snapshots of benzene during the NVT-MD simulation at T = 3,000 K

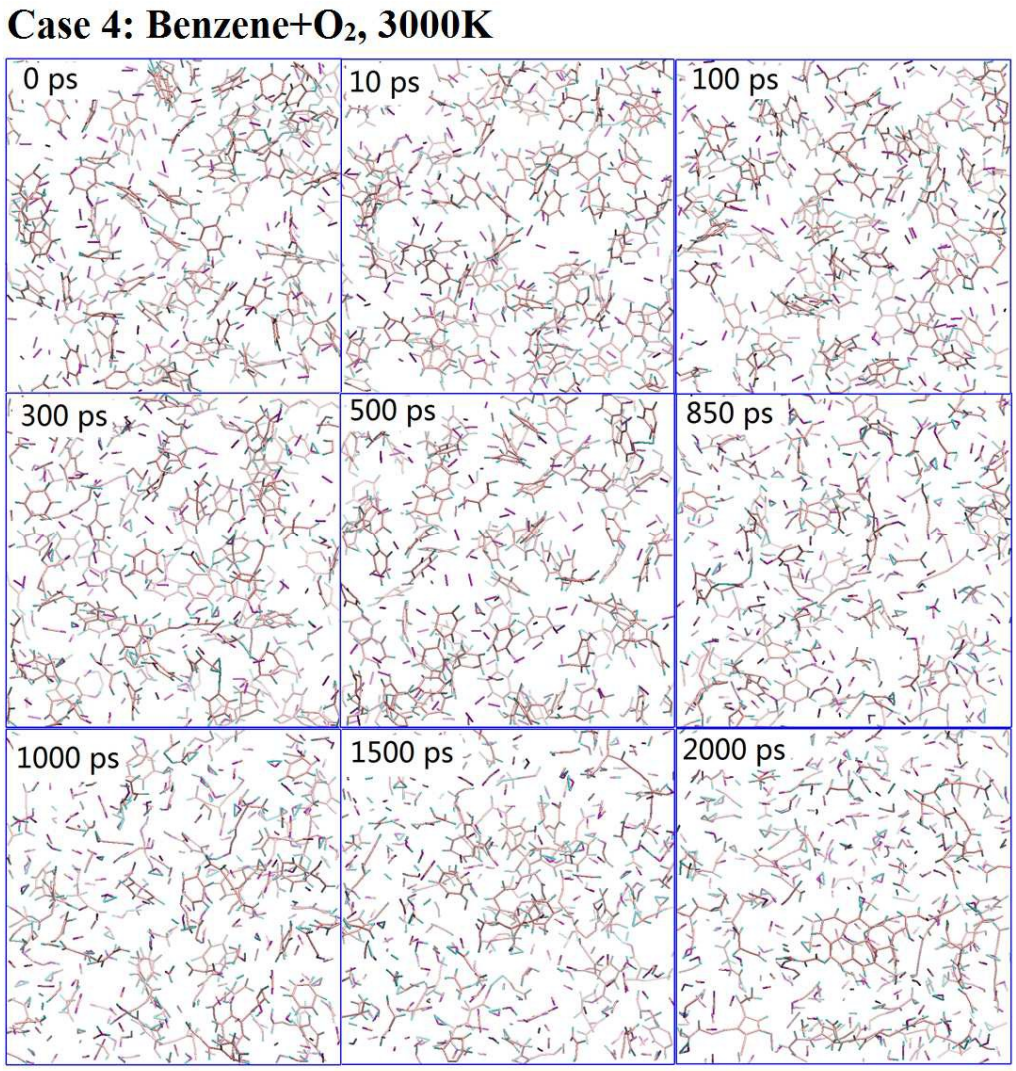

Figure 9 Snapshots of the decomposition of benzene in the presence of O_2 atmosphere during the NVT-MD simulation at T = 3,000 K

The CB growth histories can be represented by the maximal molecular weight (MW) of CBs. The evolution of MW of the CBs is shown in Figure 10. Under laser irradiation, the MWs of the CBs formed are ~3,443 (black line: 1,803 ps) and 1,018 (red line: 1,689 ps) corresponding to neat benzene and a mixture of benzene and O_2. In the neat benzene and the mixture, the largest CB were observed at 1803 ps and 1689 ps. However, as early as 101 ps, big CB with a MW of 2,839 was generated in the neat benzene. Higher C/O ratio leads to earlier large CB formation under laser

irradiation. The largest CBs are much bigger at higher C/O ratio.

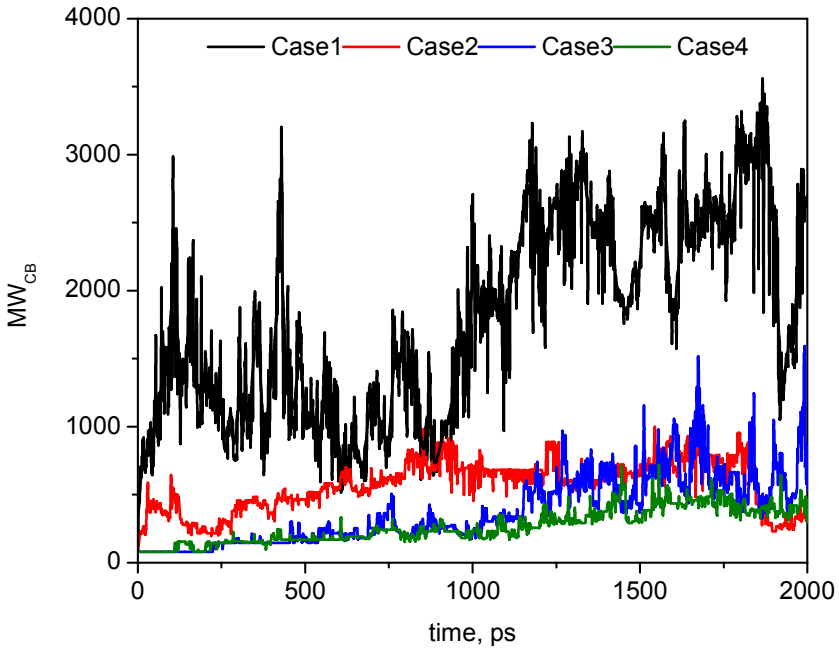

Figure 10 Evolution of maximal MW of CBs

Under a high temperature of 3,000 K, the CBs with MWs of ~1740 (black line 1992 ps) and 856 (red line 1,557 ps) were formed corresponding to the neat benzene and a mixture of benzene and O_2. In the neat benzene and mixture, the largest CB was observed at 1,992 ps and 1,557 ps, respectively. However, as early as 1,269 ps, big CB with a MW of 1,051 was generated in the neat benzene. Higher C/O ratios led to earlier large CBs formation under high temperatures. The CBs were much bigger at higher C/O ratios.

The summary of the analysis of two points is summarized. First, for a same system, laser irradiation is helpful to produce more or larger CBs in a shorter time, because the laser irradiation results in much higher temperature for complete

decomposition of benzene to generate a significant amount of dissociative carbon atoms, supplying sufficient material for the formation of CBs. Moreover, based on this, the laser irradiation of hydrocarbon fuel is considered as a feasible approach to produce some useful nanomaterials such as diamond, fullerene, graphite and nanotube, and all of which are substantially CBs. Second, no matter under laser irradiation or high temperature, higher C/O ratio is beneficial for the generation of more and larger CBs. Higher C/O ratio indicates fewer O_2, and the presence of O_2 will combine more dissociative carbon atoms to form CO_2 and CO, inhibiting the formation of CBs. As a result higher C/O ratio is beneficial for the generation of more and larger CBs.

In all these simulations, the formation of carbon cages or tubes was not observed, probably because of shorter simulating time. When the CB structure of the graphite-like lamellar is built, cages or tubes might be created if the lamellar wraps itself in a long run of simulation. This problem needs to be addressed in the near future.

4. Conclusions

In this study, we investigated the pyrolysis behaviors of benzene in the presence or absence of oxygen, by laser irradiation or simply by high temperature. The pyrolysis and combustion mechanisms of benzene under different chemical environment and temperatures were investigated by ReaxFF MD. Two systems were studied, pure benzene and a mixture of benzene and oxygen gas. The chemical behaviors induced by high-energy density laser compared to those at high temperature were investigated. Ultrahigh temperature was used to mimic laser irradiation. First,

the ReaxFF MD simulations showed that the decomposition rates of benzene were significantly accelerated by laser irradiation or in the presence of oxygen. Second, the initiation pathways were also increased by these two factors. The primary initiation pathway only involved a hydrogen atom loss in benzene pyrolysis at 3000K, and it became more complicated after the laser irradiation or in the presence of oxygen including hydrogen atom loss, cycloreversion of the ring and from the middle of the ring after reacting with an O_2 molecule. Third, the ReaxFF MD simulations formed reasonable carbon black (CB) texture of various sizes in the pyrolysis of benzene, and we also focused on the evolution of the texture of CB. The decay evolution under the aforementioned temperatures shows that both the temperature and C/O ratio mainly affected the decomposition rate of benzene. The formation of CB is very common in the partial combustion of benzene. More CBs were created in the presence of less amount of oxygen.

The calculation results of the final gaseous products, hydrocarbons, and the formation of CB are in a good agreement with the literature. This study provides a better understanding of the initiation mechanisms of the pyrolysis and combustion of benzene under extreme conditions and also obtains a direct observation of the generation of CBs at aromatic level.

Acknowledgement

We greatly appreciate the financial support from the Defense Industrial Technology Development Program（B1520132004）, the Science and Technology Innovation Fund of Institute of Chemical Materials, CAEP(No. kjcx-201305), and the National Natural Science Foundations of China (11372291 and 11372292).

Author Information

Corresponding Author, Dr. Yushi Wen, e-mail: wenys@caep.cn

Notes

The authors declare no competing financial interest.

Reference:

1. J. M. Simmie, Prog. Energy Combust. Sci., 2003. 29: p. 599–634.
2. J. A. Miller, R.J. Kee, C.K. Westbrook, Annu. Rev. Phys. Chem., 1990. 41: p. 345–387
3. H. Richter and J. B. Howar, Prog. Energy Combust. Sci., 2000. 26: p. 565–608
4. J. A. Miller, M. J. Pilling, J.Troe, Proc. Combust. Inst., 2005. 30: p. 43–88.
5. Z. Qin, V.V. Lissianski, H. Yang, W.C. Gardiner, S.G. Davis, H. Wang, Proc. Combust. Inst., 2000. 28: p. 1663–1669.
6. G. Black, H.J. Curran, S. Pichon, J.M. Simmie, V. Zhukov, Combust. Flame, 2010. 157: p. 363–373.
7. C.K. Westbrook, W.J. Pitz, O. Herbinet, H.J. Curran, E.J. Silke, Combust. Flame, 2009. 156: p. 181–199.
8. H. Wang and M. Frenklac, Combust. Flame 1997. 110: p. 173–221.
9. P. Dagaut, Phys. Chem. Chem. Phys., 2002. 4: p. 2079–2094.
10. F. Battin-Leclerc, Prog. Energy Combust. Sci., 2008. 34: p. 440–498.
11. S. Pierucci and E. Ranzi, Comput. Chem. Eng., 2008. 32: p. 805–826.
12. Q.D. Wang, J.B. Wang, J.Q. Li, N.X. Tan, X.Y. Li, Combust. Flame 2011. 158: p. 217–226
13. L. Liu, C. Bai, H. Sun, W.A. Goddard III, J. Phys. Chem. A, 2011. 115: p. 4941–4950
14. H.J. Qian, A. C. T. van Duin, K. Morokuma, and S. Irle, J. Chem. Theory. Comput., 2011. 7: p. 2040–2048.
15. R. Adams, FocusPigm, 2007. 3: p. 1-2.
16. F.J.B. Calleja, R.K. Bayer, T.A. Ezquerra, J Mater Sci, 1988. 23(4): p. 1411–1415.
17. I. Balberg, Phys. Rev. Lett. 1987. 59(12): p. 1305–1308.
18. Soboleva T, Z.X., Malek K, Xie Z, Navessin T, Holdcroft S., ACS Appl Mater Interfaces 2010. 2(2): p. 375–384.
19. B. Z. Fang, M. S. Kim, J, H, Kim, J. S. Yu, J. Am. Chem. Soc. 2009. 131: p. 15330–15338.
20. A. Guha, W.J. Lu, T.A. Zawodzinski and D.A. Schiraldi, Carbon, 2007. 45(7): p. 1506–1517.
21. Z Rigbi, Reinforcement of rubber by carbon black. Berlin/Heidelberg: Springer, 1980: p. 21–68
22. D.J. Kohls, B.G., Curr Opinion Solid State Mater Sci 2002. 6(3): p. 183–194.
23. Piasta D, Spange S, Simon F., Langmuir 2009. 25: p. 9071–9077.
24. C. K. Leong, D. D. L. Chung, Carbon 2006. 44: p. 435–440
25. Q. Li, L.D., Y. Liu, H. A. Xie, C. X. Xiong, Carbon, 2011. 49: p. 1033–1051.

26. J.B. Donnet, R.C. Bansal, M.J. Wang, Carbon black: science and technology. 2nd ed. New York: Marcel Dekker Inc.; 1993.
27. F.C. Lockwood, J.E. Van Niekerk, Combust Flame, 1995. 103: p. 76–90.
28. L. Rothbuhr, J. Witte, Process for the production of furnace black. US patent 4292291, 1979.
29. S. Ban, K. Malek, C. Huang, Z. Liu, Carbon, 2011. 49: p. 3362–3370.
30. A.D.H. Clague, J.B. Donnet, D., T.K. Wang, J.C.M. Peng, Carbon 1999. 37: p. 1553–1565.
31. M. C. Xue, D. Q. Wei., J. Q. Li, J. B. Wang, and X. Y. Li, J. Phys. Chem. A, 2012. 116(40): p. 9811–9818.
32. http://en.wikipedia.org/wiki/Benzene. 2014 access.
33. A. Tregrossi, A. Ciajolo, R. Barbella, Combustion and Flame, 1999. 117(3): p. 553–561.
34. G. Vourliotakis, G. Skevis, and M. A. Founti, Energy Fuels, 2011. 25(5): p. 1950–1963.
35. R. Addink，E.R. Altwicker, Environ. Sci. Technol., 2004. 38(19): p. 5196–5200.
36. Theodore W. Richards and Setsuro Tamaru, J. Am. Chem. Soc., 1920. 42(8): p. 1599–1617.
37. L. S. Caretto, K.N., Ind. Eng. Chem. Proc. Des. Dev., 1966. 5(3): p. 217–222.
38. S. F. Zuo, X.S., N. N. Lv, and C. Z. Qi, ACS Appl. Mater. Interfaces, 2014. 6(15): p. 11988–11996.
39. T. Yatsuhashi, N. Uchida, K. Nishikawa, Chem. Lett., 2012. 41(7): p. 722- 724.
40. A Tregrossi, A Ciajolo, R Barbella, Combustion and Flame, 1999. 117: p.553–561
41. C. D. David and H. Weichel, J. Appl. Phys., 1969. 40: p.3674-3679
42. F. J. Allen, J. Appl. Phys., 1971.42: p. 3145-3149
43. Y. Chai and L. D. Pfefferle, Fuel 1998.77: P.313–20
44. T. Cheng, A.J.-B., Goddard, W. A. III., and H. Sun, J. Am. Chem. Soc., 2014. 136(38): p. 13467–13467.
45. C. Kimberly, van Duin, A. C. T., and Goddard, W. A. III., J. Phys. Chem. A, 2008. 112(5): p. 1040–1053.
46. Agrawalla, van Duin, A. C. T., J. Phys. Chem. A 2011. 115: p. 960-972.
47. Hoover, W., Phys. Rev. A, 1985. 31: p. 1695-1697.
48. Fidel Castro-Marcanoa, Amar M. Kamatb, Michael F. Russo Jr.b, Adri C.T. van Duinb, Jonathan P. Mathewsa, Combustion and Flame, 2012. 159: p. 1272-1285.
49. S.J. Plimpton, J. Comput. Phys., 1995. 117: p. 1.
50. Aktulga, H.M.F., J. C.; Pandit, S. A.; Grama, A. Y., Parallel. Comput. 2012. 38: p. 245.
51. Strachan, van Duin, A. C. T.; Chakraborty, D.; Dasgupta, S.; Goddard, W. A. III., Phys. Rev. Lett., 2003. 91: p. 098301
52. L. A. Gribov, I. A. Novakov, A. I. Pavlyuchko, O. Yu. Shumovskii, Journal of Structural Chemistry. 2007. 48: p. 400-406.
53. Andreas A. Zavitsas, J. Phys. Chem. A 2003. 107: p.897-898
54. V. Detilleux and J. Vandooren, Combustion, Explosion, and Shock Waves, 2009.45: p. 392–403
55. B. Yang, Y. Y. Li, L. X. Wei, C. Q. Huang, J. Wang, Z. Y. Tian, R. Yang, L. S. Sheng, Y. W. Zhang, F. Qi, Proceedings of the Combustion Institute 2007.31: p. 555–563